Gene Inactivation of Proprotein Convertase Subtilisin/Kexin Type 9 Reduces Atherosclerosis in Mice

Maxime Denis, PhD; Jadwiga Marcinkiewicz, MSc; Ahmed Zaid, PhD; Dany Gauthier, BSc; Steve Poirier, PhD; Claude Lazure, PhD; Nabil G. Seidah, PhD; Annik Prat, PhD

Background—The proprotein convertase subtilisin/kexin type 9 (PCSK9) promotes independently of its enzymatic activity the degradation of the low-density lipoprotein (LDL) receptor. PCSK9 gain of function in humans leads to autosomal dominant hypercholesterolemia, whereas the absence of functional PCSK9 results in ≈7-fold lower levels of LDL cholesterol. This suggests that lowering PCSK9 may protect against atherosclerosis.

Methods and Results—We investigated the role of PCSK9 in atherosclerosis in C57BL/6 wild-type (WT), apolipoprotein E–deficient, and LDL receptor–deficient mouse models. Circulating cholesterol levels, fast protein liquid chromatography profiles, aortic cholesteryl esters (CE), and plaque sizes were determined. Intima-media thicknesses were measured by ultrasound biomicroscopy. First, mice expressing null (knockout [KO]), normal (WT), or high (transgenic [Tg]) levels of PCSK9 were fed a 12-month Western diet. KO mice accumulated 4-fold less aortic CE than WT mice, whereas Tg mice exhibited high CE and severe aortic lesions. Next we generated apolipoprotein E–deficient mice, known to spontaneously develop lesions, that expressed null (KO/e), normal (WT/e), or high (Tg/e) levels of PCSK9. After a 6-month regular diet, KO/e mice showed a 39% reduction compared with WT/e mice in aortic CE accumulation, whereas Tg/e mice showed a 137% increase. Finally, LDL receptor–deficient mice expressing no (KO/L), normal (WT/L), or high (Tg/L) levels of PCSK9 were fed a Western diet for 3 months. KO/L and Tg/L mice exhibited levels of plasma cholesterol and CE accumulation similar to those of WT/L mice, suggesting that PCSK9 modulates atherosclerosis mainly via the LDL receptor.

Conclusions—Altogether, our results show a direct relationship between PCSK9 and atherosclerosis. PCSK9 overexpression is proatherogenic, whereas its absence is protective. **(*Circulation*. 2012;125:894-901.)**

Key Words: atherosclerosis ■ cardiovascular diseases ■ cholesterol ■ lipoproteins ■ proprotein convertases

Atherosclerosis is a progressive degenerative pathology of large arteries that leads to ischemic heart diseases, which are expected to remain one of the leading causes of mortality until at least 2030.[1] The different stages of atherosclerotic plaque development have been reviewed extensively.[2–5] In brief, high levels of circulating atherogenic lipoproteins favor the accumulation of oxidized low-density lipoproteins (LDLs) in the subendothelial space. The latter are taken up by invading macrophages that, if they cannot efflux excess cholesterol to high-density lipoprotein, become foam cells. Foamy cells then release cytokines that recruit more macrophages into the building plaque. After formation of a necrotic core, plaques may ultimately become unstable; their fibrous cap can rupture and cause the formation of thrombus that can lead to death. Although inflammation is an important contributor to atherosclerosis, accumulation of oxidized LDLs in the subendothelial compartment is a key triggering event in atherosclerosis. Lowering the levels of circulating atherogenic particles is thus a good approach to prevent cardiovascular diseases.

Clinical Perspective on p 901

Autosomal dominant hypercholesterolemia is a disorder of elevated plasma levels of LDL cholesterol (LDL-C) linked to dominant mutations occurring mostly in the gene encoding the LDL receptor (LDLR) and less frequently in that encoding apolipoprotein B. In 2003, a third locus involved in familial hypercholesterolemia was discovered,[6] the *PCSK9* gene encoding the proprotein convertase subtilisin/kexin type 9 (PCSK9).[7] This serine protease belongs to the family of proprotein convertases (PCs) that cleave precursors of hormones, growth factors, receptors, or membrane-bound transcription factors (for review, see Seidah et al[8]). However,

Received July 25, 2011; accepted December 28, 2011.

From the Laboratory of Biochemical Neuroendocrinology (M.D., J.M., A.Z., S.P., N.G.S., A.P.) and Laboratory of Neuropeptide Structure and Metabolism (D.G., C.L.), Clinical Research Institute of Montreal, Montreal, Canada. Dr Zaid is presently at the Department of Biochemistry, Faculty of Medicine, Tripoli University, Tripoli, Libya.

The online-only Data Supplement is available with this article at http://circ.ahajournals.org/lookup/suppl/doi:10.1161/CIRCULATIONAHA.111.057406/-/DC1.

Correspondence to Annik Prat, PhD, Laboratory of Biochemical Neuroendocrinology, Clinical Research Institute of Montreal, 110 Pine Ave W, Montreal, QC, H2W 1R7, Canada. E-mail prata@ircm.qc.ca

unlike the other PCs, PCSK9 has thus far no known substrate but itself. In the endoplasmic reticulum, it autocatalytically cleaves its prosegment, which remains noncovalently tightly bound to the protein.[7,9] Several studies have now clearly established that PCSK9 regulates LDLR protein levels. In a complex with its prosegment, PCSK9 binds the LDLR and prevents recycling of the receptor to the cell surface, thereby promoting its degradation in lysosomes.[9–11] A recent study suggests that PCSK9 binding maintains 3 contiguous domains of the LDLR (L7, repeat 7 of the ligand binding domain; EGF-A; EGF-B) in an extended conformation that is incompatible with LDLR recycling to the cell surface.[12] However, PCSK9 binding to the LDLR may also be regulated by other partners, namely, via interactions involving the cysteine- and histidine-rich C-terminal domain of PCSK9.[13] PCSK9 is highly expressed in the liver and is found in the plasma at concentrations of ≈100 to 200 ng/mL.[14,15] Although PCSK9 is a key player in cholesterol homeostasis through the regulation of LDLR levels, circulating PCSK9 also plays a role in triglyceride metabolism by promoting the degradation of the very low-density lipoprotein (VLDL) receptor.[16–18] In addition, PCSK9 promotes ex vivo the degradation of apolipoprotein ER2,[16,17] which is also closely related to the LDLR.

Approximately 2% to 3% of patients with autosomal dominant hypercholesterolemia carry mutations in PCSK9. Gain-of-function mutations of the human PCSK9 protein lead to higher circulating LDL-C and increased incidence of cardiovascular diseases.[19] The most severe mutation, which was reported in Norwegians[20] and Mormons from Utah[21] who exhibit cholesterol levels of ≈500 mg/dL, is the substitution of Asp_{374} by Tyr (D374Y), which increases the affinity of PCSK9 for the LDLR by at least 10-fold.[22] Conversely, PCSK9 loss-of-function mutations lead to hypocholesterolemia. Interestingly, ≈2% of blacks carry a Y142X or C679X nonsense polymorphism in 1 *PCSK9* allele[23] that reduces LDL-C by 40%. Moreover, the characterization of 2 women lacking functional PCSK9 and exhibiting ≈14 mg/dL (0.38 mmol/L) of LDL-C revealed that PCSK9 is not essential.[24,25] Thus, PCSK9 appears to be a promising target to reduce LDL-C levels.

Statins inhibit cholesterol synthesis and increase LDLR expression in hepatocytes, thereby leading to increased hepatic LDL clearance from the circulation. However, statins concomitantly induce PCSK9 expression,[15,26] which promotes the degradation of the LDLR and thus impairs the optimal LDLR-mediated LDL clearance. Thus, PCSK9 inhibition, alone or in combination with statins, has emerged as a potentially new approach to reduce circulating LDL.

In this study, we analyzed the impact of the absence or overexpression of PCSK9 on atherosclerosis in well-established mouse models. Our data demonstrate a direct relationship between PCSK9 and the development of atherosclerosis. The accumulation of cholesteryl esters (CE) in aortas was markedly reduced in mice lacking PCSK9 in both wild-type (WT) and atherogenic apolipoprotein E (apoE)–deficient backgrounds. Conversely, PCSK9 overexpression severely worsened the atherosclerotic phenotypes. Finally, the process by which PCSK9 enhances atherosclerosis appears to be mediated primarily through its action on the LDLR because LDLR-deficient mice lacking or overexpressing PCSK9 do not show significant differences in CE accumulation and plaque size.

Methods

Animals and Diets

All procedures were approved by the animal care committee of the Institut de recherches cliniques de Montréal. $Pcsk9^{-/-}$ (knockout [KO]) mice, which lack the *Pcsk9* proximal promoter and exon 1 region, and transgenic (Tg) mice, which express murine PCSK9 under the control of the *apoE* promoter, were described previously[27] and were since backcrossed 7 to 10 times to C57BL/6 mice. C57BL/6, $Apoe^{-/-}$,[28] and $Ldlr^{-/-}$[29] mice were obtained from the Jackson Laboratory. The latter were all in a C57BL/6 background. PCSK9 KO and Tg mice were crossed to $Apoe^{-/-}$ mice or $Ldlr^{-/-}$ mice to obtain $Pcsk9^{-/-}$ $Apoe^{-/-}$ (KO/e) or $Pcsk9^{-/-}$ $Ldlr^{-/-}$ (KO/L); $Pcsk9^{+/+}$ $Apoe^{-/-}$ (WT/e) or $Pcsk9^{+/+}$ $Ldlr^{-/-}$ (WT/L); and $Tg(Pcsk9)^{+/0}$ $Apoe^{-/-}$ (Tg/e) or $Tg(Pcsk9)^{+/0}$ $Ldlr^{-/-}$ (Tg/L) mice. All transgenic strains are hemizygous for the PCSK9 transgene. At 3 to 4 weeks of age, mice were weaned and fed a regular (2018 Teklad Global) or Western (TD.88137 Harlan Teklad) diet for 3, 6, or 12 months. The Western diet contained 34%, 21%, and 0.2% of sugar, fat, and cholesterol, respectively, whereas the regular diet contained 5%, 6%, and 0% of these ingredients. PCSK9 mRNA was quantified by reverse transcription quantitative polymerase chain reaction.[27] The levels of circulating PCSK9 and of total and surface LDLR in hepatocytes were assessed by enzyme-linked immunosorbent assay, Western blotting, and immunofluorescence, respectively. These results and corresponding methods can be found in Figure I in the online-only Data Supplement.

Genotyping

Apoe, *Ldlr*, and *Pcsk9* genotyping was performed by polymerase chain reaction amplification on genomic DNA isolated from mouse tails. Polymerase chain reaction products were then separated on a 3130Xl Genetic Analyzer (Applied Biosystems) and identified on the basis of fragment size and expected fluorescence, according to the manufacturer's instructions. For the V5-tagged PCSK9 transgene,[27] a quantitative polymerase chain reaction with the use of a TaqMan probe was performed in a ViiA7 quantitative polymerase chain reaction apparatus (Applied Biosystems) in accordance with the manufacturer's instructions. The primers used are presented in the Table in the online-only Data Supplement.

Animal Euthanasia and Dissection

Mice were fasted for ≈4 hours before euthanasia. Under anesthesia with 2% isoflurane in oxygen, total bleed was performed by heart puncture with the use of a 21-gauge needle mounted on a 1-mL syringe. The right atrium was cut out, and the remaining blood was flushed by pump-monitored perfusion (0.4 mL/min) from the left ventricle with phosphate-buffered saline (PBS) for 10 minutes with the use of a 25-gauge butterfly needle mounted on a 20-mL syringe. Aortas were then perfused-fixed for 10 minutes with PBS containing 4% paraformaldehyde. Organs were weighed, and the aorta was roughly dissected from the heart down to the iliac branches and stored in 4% paraformaldehyde for 1 to 3 days. Finally, a fine dissection under a microscope further allowed removal of the adventitia before photography and lipid extraction.

Ultrasound Biomicroscopy

On the day of euthanasia, intima-media thickness (IMT) was determined by B-mode ultrasonography with a Vevo 770 apparatus (Visual Sonics, Toronto, Canada) equipped with a 30-MHz probe,[30] with a depth focus at 12.7 mm. Animals were maintained under anesthesia with 2% isoflurane in oxygen during the whole procedure. A hair remover (Nair) was used to clean the mouse chest, and a transmission gel was applied before scanning. Three-second cine-

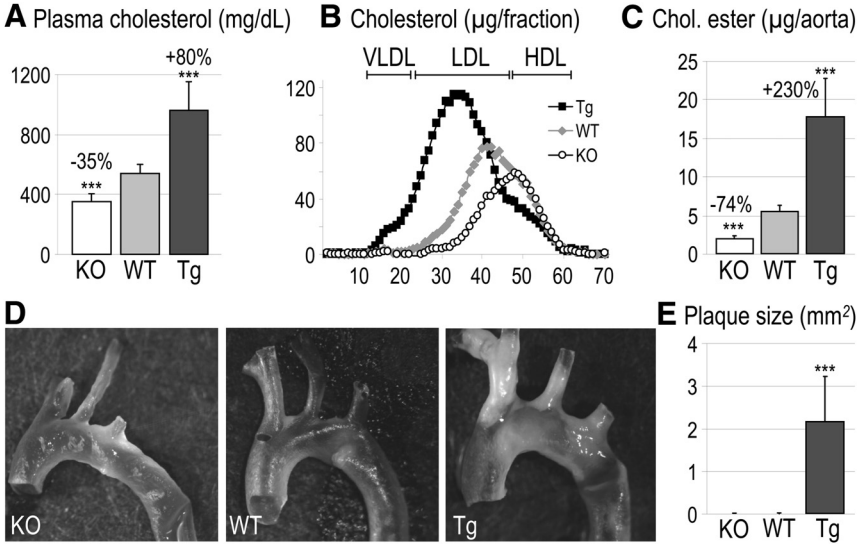

Figure 1. Direct relationship between atherosclerosis and proprotein convertase subtilisin/kexin type 9 (PCSK9) in mice. C57BL/6 male mice that express no PCSK9 (knockout [KO]), normal levels (wild-type [WT]), and high levels of murine PCSK9 (transgenic [Tg]) were fed a Western diet for 12 months (n=5–6 mice per genotype). **A**, Plasma cholesterol. **B**, Fast protein liquid chromatography cholesterol profiles (pooled plasma); very low-density lipoprotein (VLDL), low-density lipoprotein (LDL), and high-density lipoprotein (HDL) fractions are indicated. **C**, Cholesteryl (Chol.) ester accumulation in the whole aorta. **D**, Representative en face preparations of aortic arches. **E**, Cumulative plaque size at the level of aortic valves and root. Bars and error bars represent mean±SD; by comparison with WT values, P (***$P \leq 0.001$) was obtained with a 2-tailed Student t test.

loop movies were recorded for further offline analysis. A left parasternal long-axis view was used to visualize the aortic valves, aortic root, and ascending aorta. A right parasternal short-axis view was used to visualize the aortic arch and brachiocephalic artery (Figure II in the online-only Data Supplement). All measurements were performed at systole by an operator blinded for genotypes. The measurement at the level of the valves was taken as a perpendicular cross section directly in the middle of the valves; for the aortic root, the measurement was taken at the level of the coronary branches; for the ascending aorta, it was taken ≈1 mm away from the beginning of the aortic root; and for the brachiocephalic artery, the measurement was taken ≈0.5 mm away from the branching from the aortic arch. IMT was defined as follows: (outer diameter−inner diameter)/2.

Plasma Cholesterol Analysis

Blood was stored on ice in Eppendorf tubes containing 15 µL of 40 U/mL heparin, centrifuged at 3000 rpm for 20 minutes at 4°C, and the supernatant was frozen until further analysis. For fast protein liquid chromatography (FPLC) profiles, plasma samples from 5 to 10 mice were combined, and 400 µL was loaded on a 10×60-mm Superose 6 column eluted with 0.9% NaCl, pH 7.0, at a rate of 300 µL/min in 96 fractions. Total cholesterol in the original plasma (4 µL) or in FPLC fractions (125 or 75 µL of 300 µL for regular or Western diet, respectively) was determined with the use of the Infinity kit.

Aortic Lipid Extraction and CE Determination

The aorta was cut into small pieces with microscissors, crushed in 250 µL PBS with homogenizers for Eppendorf tubes, and further homogenized by passing 20 times in a 25-gauge needle mounted on a 1-mL syringe. The volume was completed to 500 µL with PBS, and the sample was sonicated 3×10 seconds on ice. After transfer in a glass tube, 4.5 mL of methanol/chloroform (1:2) was added, and samples were incubated overnight with vigorous agitation. Samples were centrifuged at 1000g for 10 minutes, the aqueous (upper) phase was removed, the organic (lower) phase was transferred to a new glass tube and evaporated under a nitrogen atmosphere, and 450 µL of 1% Triton X-100 in chloroform was added before final evaporation. Determination of CE levels was then performed as described[31] with slight modifications. Briefly, lipids were resuspended in 225 µL of water. For total or free cholesterol measurements, 10 to 50 µL per well was loaded on a 96-well plate together with a set of known cholesterol standards (0–25 µg). Total cholesterol values were obtained at 450 nm with the use of 200 µL per well of the Infinity (Thermo Fisher Scientific) reagent, and free cholesterol values were determined at 550 nm with the use of 200 µL per well of the free cholesterol E (Wako) reagent. CE/aorta values were determined as total cholesterol/aorta−free cholesterol/aorta.

Histological Quantification of Plaques

After perfusion-fixation, the upper part of the heart was separated from the ascending aorta, further fixed overnight in 4% paraformaldehyde in PBS, and embedded in paraffin. From the beginning of the valves to the aortic root (≈420 µm), 6 slices were analyzed (1 every 70 µm) for determination of plaque area after Verhoeff/van Gieson staining. Plaques were manually outlined by an observer blinded for mouse genotypes with the use of ImageJ Software after adjustment for pixel size. Neighboring sections stained with Masson's trichrome were selected for publication.

Statistical Analysis

Mean±SD values are presented except for ultrasound biomicroscopy, for which mean±SEM values are shown. Two-tailed Student t tests rather than ANOVA tests were performed to determine P values because our ultimate goal was to compare KO versus WT mice and Tg versus WT mice.

Results

PCSK9 Deficiency Protects Mice Fed a Western Diet From Atherosclerosis

C57BL/6 mice expressing null (KO), normal (WT), or high (Tg) hepatic PCSK9 levels have been described previously.[27] In the present study, their plasma and liver were further analyzed by PCSK9 enzyme-linked immunosorbent assay, quantitative polymerase chain reaction, immunoblotting, and immunofluorescence (Figure I in the online-only Data Supplement). Compared with WT mice, Tg mice have >100 times increased hepatic PCSK9 mRNA levels, 9-fold more circulating total PCSK9, undetectable cell surface LDLR in liver sections, and a 77% reduction in total liver LDLR protein. To assess the role of PCSK9 in atherogenesis, we first rendered these mice moderately dyslipidemic by feeding them a Western diet enriched in cholesterol, sugar, and fat (see Methods). KO mice fed a Western diet for 12 months, compared with WT mice fed the same diet, had a 35% reduction in plasma cholesterol levels associated with lower LDL-C levels (Figure 1A and 1B). KO mice also exhibited a 74% reduction in aortic CE (Figure 1C) to reach the CE levels

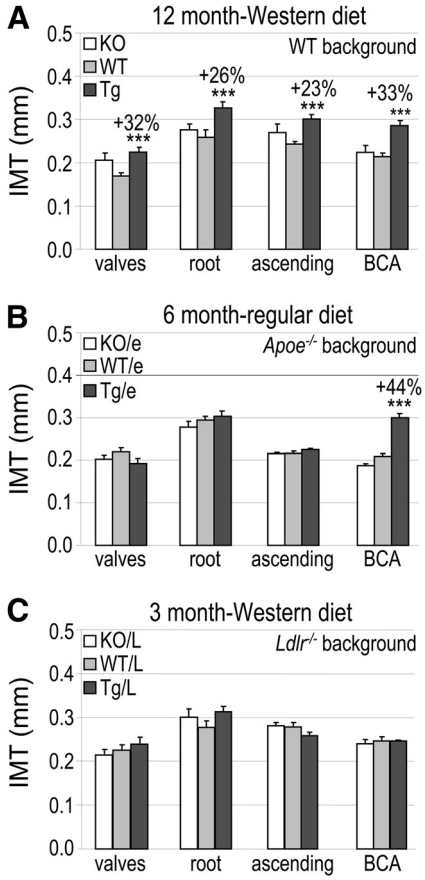

Figure 2. Analysis of intima-media thickness (IMT). IMT was determined at the level of aortic valves and root, in the ascending aorta, and in the brachiocephalic artery (BCA) by ultrasound biomicroscopy. **A**, Proprotein convertase subtilisin/kexin type 9 (PCSK9) knockout (KO), wild-type (WT), or transgenic (Tg) mice fed a Western diet for 12 months (n=5). **B**, Apolipoprotein E (apoE)–deficient mice expressing either no (KO/e), normal (WT/e), or high (Tg/e) levels of PCSK9 fed a regular diet for 6 months (n=10–12). **C**, Low-density lipoprotein receptor (LDLR)–deficient mice expressing either no (KO/L), normal (WT/L), or high (Tg/L) levels of PCSK9 fed a Western diet for 3 months (n=8–10). Bars and error bars represent mean±SD; by comparison with corresponding WT values (gray bars), *P* (***$P \leq 0.001$) was obtained with a 2-tailed Student *t* test.

usually observed in mice fed a chow diet (not shown), suggesting that the absence of PCSK9 abolished the diet-induced aortic CE accumulation. As reported previously,[32] WT mice fed a Western diet exhibited no detectable lesions by en face preparation (Figure 1D), histological analysis (Figure 1E and Figure IIIA in the online-only Data Supplement), and ultrasound biomicroscopy (Figure 2A). In contrast, Tg mice fed a Western diet for 12 months exhibited a marked increase in plasma cholesterol (+80%; Figure 1A) and aortic CE (+230%; Figure 1C). They were also the only mice that developed visible lesions, as assessed by en face preparation (Figure 1D), histological analysis (Figure 1E and Figure IIIA in the online-only Data Supplement), and ultrasound biomicroscopy (Figure 2A). Therefore, a direct relationship was observed between PCSK9 expression levels and aortic CE accumulation in mice fed a Western diet for 12 months. However, a potentially beneficial effect of the absence of PCSK9 on the development of advanced lesions could not be assessed with this approach.

PCSK9 Deficiency Protects ApoE-Deficient Mice From Atherosclerosis

The effect of PCSK9 on atherosclerosis was next examined in apoE-deficient mice known to spontaneously develop advanced lesions, even when fed a regular diet.[32,33] ApoE-deficient mice expressing either no PCSK9 (KO/e; ie, $Pcsk9^{-/-}$ $Apoe^{-/-}$), normal levels of PCSK9 (WT/e; ie, $Pcsk9^{+/+}$ $Apoe^{-/-}$), or high levels of murine PCSK9 [Tg/e; ie, $Tg(Pcsk9)^{+/0}$ $Apoe^{-/-}$] were fed a regular diet for 6 months, and their LDLR and PCSK9 levels were characterized (Figure I in the online-only Data Supplement). Different from WT mice fed a Western diet (Figure 1B), $Apoe^{-/-}$ mice exhibited a huge accumulation of VLDL remnants and LDL (Figure 3B), as expected from the known key role of apoE in mediating lipoprotein binding to receptors.[33] Possibly because of a dominant effect of apoE deficiency, plasma cholesterol levels were not significantly affected by the loss or overexpression of PCSK9 (Figure 3A). However, the aortic CE content was reduced by 39% in KO/e mice and increased by 137% in Tg/e mice (Figure 3C). Moreover, the latter mice exhibited a highly significant 207% increase of the average plaque size (Figure 3E). En face preparations of aortas (Figure 3D) showed more plaques in Tg/e mice. With the use of ultrasound biomicroscopy, no differences were detected between genotypes at the level of the root and ascending aorta, but a reliable 44% increase of IMT in the brachiocephalic artery was observed in Tg/e mice (Figure 2B). Although KO/e and Tg/e plasma cholesterol levels were not significantly different from those of WT/e mice (Figure 3A), a trend for lower intermediate-density lipoprotein/LDL-C levels was observed in KO/e mice and an opposite trend for higher intermediate-density lipoprotein/LDL-C levels in Tg/e mice (Figure 3B), consistent with the known ability of PCSK9 to trigger LDLR degradation.

Effect of Age, Gender, and Diet in the ApoE-Deficient Background

Groups of KO/e, WT/e, and Tg/e mice were also fed a regular diet for 3 and 12 months. Three months after weaning, aortic CE was not markedly different between genotypes. After 12 months, however, aortic CE contents were ≈4-fold higher than those obtained after 6 months (Figure 4), showing an exponential accumulation with time in all genotypes. Importantly, the degree of protection due to the absence of PCSK9 (32% versus 39% after 6 months; KO/e) remained in the same range, as well as the degree of exacerbation due to PCSK9 overexpression (167% versus 137% after 6 months; Tg/e). Analysis of groups of female mice fed a regular diet for 6 months revealed results similar to those observed in groups of males (Figure IV in the online-only Data Supplement), showing that the proatherogenic effect of PCSK9 is not sex dependent. Finally, apoE-deficient mice were also fed a Western diet for 6 months, which caused the approximate doubling of plasma cholesterol values in all genotypes (not shown). KO/e mice were still protected from aortic CE accumulation (−19%), and their IMT was significantly re-

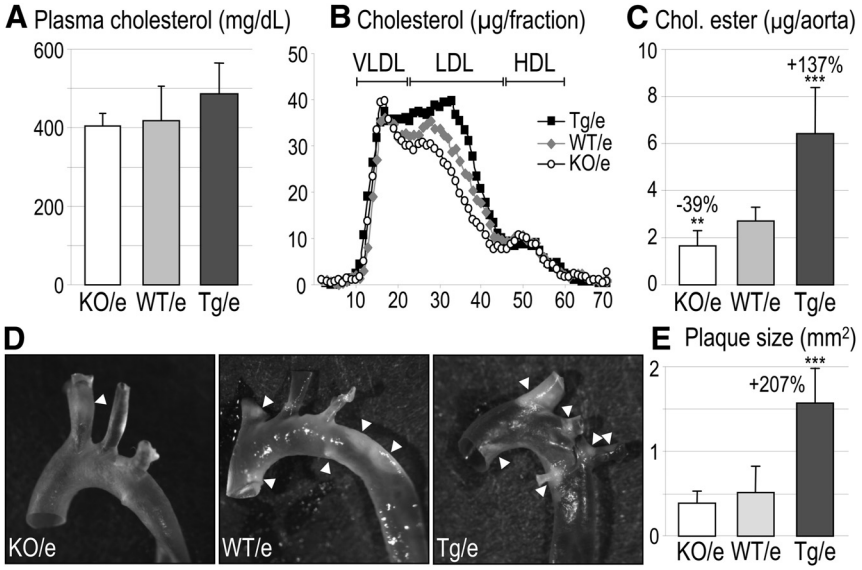

Figure 3. The absence of proprotein convertase subtilisin/kexin type 9 (PCSK9) protects apolipoprotein E (apoE)–deficient mice from atherosclerosis. ApoE-deficient male mice expressing null (knockout [KO]/e), normal (wild-type [WT]/e), or high (transgenic [Tg]/e) levels of PCSK9 were fed a normal diet for 6 months. **A**, Plasma cholesterol (n=10–13). **B**, Fast protein liquid chromatography cholesterol profiles (pooled plasma from 10 mice per genotype). **C**, Cholesteryl (Chol.) ester accumulation in the whole aorta (n=11–15). **D**, Representative en face preparations of aortic arches. **E**, Cumulative plaque surface at the level of aortic valves and root (n=9–15). Bars and error bars represent mean±SD; by comparison with WT/e values, *P* (***P*≤0.01; ****P*≤0.001) was obtained with a 2-tailed Student *t* test.

duced at the level of the aortic valves (−25%), root (−18%), and ascending aorta (−9%) in KO/e mice (Figure V in the online-only Data Supplement). However, no significant decrease of the plaque size was observed. Conversely, Tg/e mice had higher CE contents (+50%) and plaque size (+28%) and significantly higher IMT at the level of ascending aorta (+19%) and brachiocephalic artery (+40%). Altogether, our results suggest that the absence of PCSK9 protects apoE-deficient mice against atherosclerosis in both males and females, even when fed a Western diet.

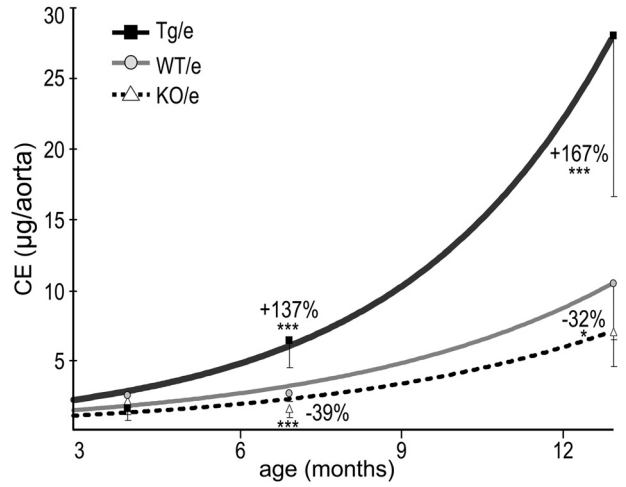

Figure 4. Time course study of the protective effect of proprotein convertase subtilisin/kexin type 9 (PCSK9) in apolipoprotein E (apoE)–deficient mice. ApoE-deficient male mice expressing null (knockout [KO]/e), normal (wild-type [WT]/e), or high (transgenic [Tg]/e) PCSK9 levels were fed a normal diet for 3, 6, or 12 months from weaning (at ≈1 month of age) to euthanasia at 4, 7, or 13 months of age, respectively. Cholesteryl ester (CE) contents (mean±SD) of aortas were determined (n=10–12 mice per point). Note that data at 7 months correspond to those presented in Figure 3C. Symbols and error bars represent mean−SD; by comparison with WT/e values, *P* (**P*≤0.05; ****P*≤0.001) was obtained with a 2-tailed Student *t* test. Least squares fit exponential curves were obtained with the use of GraphPad Prism Software (version 5.04); r^2=0.71, 0.69, and 0.78 for KO/e, WT/e, and Tg/e curves, respectively.

PCSK9 Regulates Circulating Cholesterol and Aortic CE Accumulation via the LDLR

PCSK9 regulates LDLR[10] and VLDLR levels in vivo[18] and may affect other targets. To evaluate the role of PCSK9 in atherogenesis in the absence of the LDLR, LDLR-deficient mice lacking PCSK9 (KO/L; $Pcsk9^{-/-}$ $Ldlr^{-/-}$) or expressing normal (WT/L; $Pcsk9^{+/+}$ $Ldlr^{-/-}$) or high [Tg/L; $Tg\text{-}(Pcsk9)^{+/0}$ $Ldlr^{-/-}$] levels of murine PCSK9 were fed a Western diet for 3 months. The 3 lines did not significantly differ in plasma cholesterol, FPLC profiles, CE, en face plaque accumulation, plaque size (Figure 5), and IMT (Figure 2C). These results indicate that PCSK9 exerts its effect on atherosclerosis mainly via the LDLR.

Discussion

In the present study, we compared the effects of the inactivation of PCSK9 versus its overexpression in the liver on the development of atherosclerosis in mice. We showed for the first time that the absence of PCSK9 protects WT and apoE-deficient mice from atherosclerosis, whereas PCSK9 overexpression results in stronger atherosclerotic phenotypes. Our data are in agreement with the reported 88% lower risk of developing cardiovascular complications over a 15-year period in individuals lacking 1 functional PCSK9 allele,[34] as well as with the reported atherogenic effect of human PCSK9-D374Y overexpression in mice.[35]

In our study, atherosclerosis was tracked by 3 different but complementary techniques: (1) histological determination of plaque size at the level of the aortic valves and root; (2) ultrasound biomicroscopy at the level of aortic valves, root, ascending aorta, and brachiocephalic artery; and (3) CE accumulation in the whole aorta. Some discrepancies were observed between techniques and across the various models of mice used here. Those are mainly due to the specific regions examined and to the inherent sensitivity of each technique. Although histological analysis is a direct assessment, it is restricted to the aortic valves and root and did not allow detection of low levels of lipid accumulation in the remainder of the aorta (Figure 1E). Ultrasound biomicros-

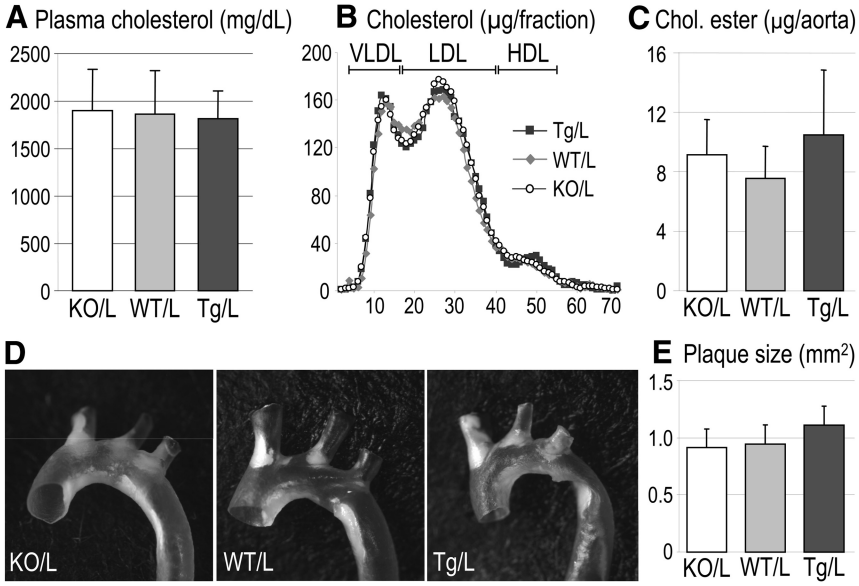

Figure 5. Proprotein convertase subtilisin/kexin type 9 (PCSK9) modulates atherosclerosis essentially via the low-density lipoprotein receptor. Low-density lipoprotein receptor–deficient mice expressing null (knockout [KO]/e), normal (wild-type [WT]/e), or high (transgenic [Tg]/e) PCSK9 levels were fed a Western diet for 3 months. **A**, Plasma cholesterol (n=7–15). **B**, Fast protein liquid chromatography cholesterol profiles (pooled plasma from 6–9 mice per genotype). **C**, Cholesteryl (Chol.) ester accumulation in the whole aorta (n=7–13). **D**, Representative en face preparations of aortic arches. **E**, Cumulative plaque surface at the level of aortic valves and root (n=7–9). Bars and error bars represent mean±SD.

copy, although noninvasive and rapid, did not detect subtle changes that were seen by CE determination (Figure 2B versus Figure 3C). In contrast, despite requiring special dissection skills and patience, the determination of whole aortic CE contents was the most reliable assessment of the progression of atherosclerosis of the whole aorta, from early to late stages of plaque development, as observed by Véniant et al.[36]

In mice exhibiting a WT background (Figure 1) and fed a 12-month Western diet, the absence or overexpression of PCSK9 has a strong impact on LDL accumulation (−35% and +80%, respectively) and aortic CE levels (−74% and +230%, respectively). In addition, in this model that does not develop plaques spontaneously, PCSK9 overexpression resulted in abundant plaques (≈2 mm^2) and significantly increased IMTs (Figure 2A).

In apoE-deficient mice fed a 6-month regular diet (Figure 3), the absence or overexpression of PCSK9 had a lower but still measurable impact on CE accumulation, with −39% and +137% changes, respectively. Tg/e plaque size increased by 207%, whereas WT/e and KO/e plaque size did not significantly differ (0.4–0.5 mm^2). The method may not be sensitive enough to accurately detect small variations among samples at this level of plaque development. Aortic CE values seem more sensitive, but they may not reflect the extent of plaque formation across models. Indeed, although WT mice accumulated 5 µg of aortic CE without any detectable plaque (Figure 1C and 1E), a 3-µg accumulation in WT/e mice (twice younger and fed a regular instead of a Western diet) coincided with the presence of plaques (Figure 3C and 3E). ApoE deficiency thus favors the development of atherosclerotic plaques at lower CE levels.

In the apoE-deficient model, VLDL-C and LDL-C levels seem to poorly predict the development of atherosclerosis because they differed only slightly between KO/e, WT/e, and Tg/e mice. It is still unclear whether the slightly higher LDL-C levels seen in Tg/e FPLC profiles are directly responsible for the 3-fold increase in Tg/e plaque size.

The clearly attenuated atherosclerotic phenotypes observed in KO and KO/e mice suggest that loss of PCSK9 may be even more protective against atherosclerosis in humans. Indeed, (1) only 30% of the circulating cholesterol is associated with LDL-C in mice versus 70% in humans; and (2) only 30% (versus 100% in human) of apolipoprotein B–containing lipoproteins secreted from mouse liver bind the LDLR as they carry apolipoprotein B_{100}. Patients exhibiting a functional defect in apoE (type III hyperlipidemia) should also benefit from PCSK9 inhibitors.

Finally, to determine to which extent the atherogenic properties of PCSK9 were LDLR dependent, we analyzed mice exhibiting a LDLR-deficient background and fed a 3-month Western diet (Figure 5). The absence or overexpression of PCSK9 had no significant impact on circulating cholesterol, FPLC profiles, aortic CE levels, or plaque size (≈1 mm^2), suggesting that all of these parameters, and thus PCSK9 atherogenic properties, are essentially LDLR dependent. Clinically, these data suggest that patients with autosomal dominant hypercholesterolemia having no functional LDLR should not respond to a PCSK9 inhibitor.

In this study, we noted that our Tg mice that express high levels of PCSK9[18,27] and exhibit low LDLR protein levels in the liver[27] (Figure IB in the online-only Data Supplement) were by far less sensitive to atherosclerosis than LDLR-deficient mice (WT/L or *Ldlr*$^{-/-}$; Figure VI in the online-only Data Supplement). The LDLR fraction resistant to PCSK9 in Tg mice seems thus to play a key role in attenuating the atherosclerotic phenotypes. Because PCSK9 mainly exerts its effect on the LDLR either in a post-Golgi compartment or at the cell surface,[37,38] this fraction, which is likely intracellular, could be sufficient to reduce VLDL secretion via intracellular apolipoprotein B degradation.[39,40] Moreover, extrahepatic LDLR, which represents ≈30% of the whole-body LDLR,[41] may be less sensitive than hepatic LDLR to circulating PCSK9[42,43] and contribute to VLDL and LDL uptake in Tg but not in *Ldlr*$^{-/-}$ mice.

Over the last few years, it became clear that PCSK9 is a promising and likely safe target to treat hypercholesterolemia

and prevent coronary artery disease.[37] Because of its effect on VLDLR, PCSK9 inhibition could also affect the treatment of mixed dyslipidemias associated with the metabolic syndrome and diabetes mellitus. It may incidentally reduce vascular exposure to postprandial triglyceride-rich lipoproteins and prevent hepatic steatosis, as suggested from mouse studies.[18]

Our study demonstrated that a life-long reduction in LDL-C in mice is safe and protects against atherosclerosis. In view of the selectivity of action of PCSK9 on LDLR in the liver[7,27] and possibly in the small intestine,[7] it is expected that drugs that would target PCSK9 will exhibit fewer side effects that those related to statins. Various strategies were proposed to inhibit the function and/or levels of PCSK9, including mRNA knockdown approaches[44,45] or passive immunization with the use of monoclonal antibodies that inhibit binding of PCSK9 to the LDLR.[46] All of these approaches are now being tested in clinical trials[47] (http://www.clinicaltrials.gov/ct2/results?term=PCSK9), and in 2012–2013 we should know their efficacy and safety profiles. With the rapid pace of discoveries in the field, it is hoped that within a few years lead molecules reducing the level or activity of PCSK9 will be uncovered and that these will find their way into the clinic to help patients suffering from dyslipidemia and atherosclerosis.

Acknowledgments

The authors would like to acknowledge Anna Roubtsova, Claudia Toulouse, Dominic Filion, Annie Vallée, Geneviève Brindle, Manon Laprise, Antoine Enfissi, and Odile Neyret for their excellent technical support.

Sources of Funding

This work was supported by the Canadian Institutes of Health Research grants 82946 (to Drs Seidah and Prat) and 102741 (to Drs Seidah and Prat) and Canada Research Chair grant 216684 (Dr Seidah). Dr Denis was supported by a fellowship from the Heart and Stroke Foundation of Canada, Dr Poirier by a Frederick Banting and Charles Best Canada Graduate Scholarship, and Dr Zaid by the National Academy for Scientific Research.

Disclosures

None.

References

1. Mathers CD, Loncar D. Projections of global mortality and burden of disease from 2002 to 2030. *PLoS Med*. 2006;3:e442.
2. Stary HC, Chandler AB, Glagov S, Guyton JR, Insull W Jr, Rosenfeld ME, Schaffer SA, Schwartz CJ, Wagner WD, Wissler RW. A definition of initial, fatty streak, and intermediate lesions of atherosclerosis: a report from the Committee on Vascular Lesions of the Council on Arteriosclerosis, American Heart Association. *Arterioscler Thromb*. 1994;14:840–856.
3. Stary HC, Chandler AB, Dinsmore RE, Fuster V, Glagov S, Insull W Jr, Rosenfeld ME, Schwartz CJ, Wagner WD, Wissler RW. A definition of advanced types of atherosclerotic lesions and a histological classification of atherosclerosis: a report from the Committee on Vascular Lesions of the Council on Arteriosclerosis, American Heart Association. *Circulation*. 1995;92:1355–1374.
4. Lusis AJ. Atherosclerosis. *Nature*. 2000;407:233–241.
5. Libby P. Inflammation in atherosclerosis. *Nature*. 2002;420:868–874.
6. Abifadel M, Varret M, Rabes JP, Allard D, Ouguerram K, Devillers M, Cruaud C, Benjannet S, Wickham L, Erlich D, Derre A, Villeger L, Farnier M, Beucler I, Bruckert E, Chambaz J, Chanu B, Lecerf JM, Luc G, Moulin P, Weissenbach J, Prat A, Krempf M, Junien C, Seidah NG, Boileau C. Mutations in PCSK9 cause autosomal dominant hypercholesterolemia. *Nat Genet*. 2003;34:154–156.
7. Seidah NG, Benjannet S, Wickham L, Marcinkiewicz J, Jasmin SB, Stifani S, Basak A, Prat A, Chretien M. The secretory proprotein convertase neural apoptosis-regulated convertase 1 (NARC-1): liver regeneration and neuronal differentiation. *Proc Natl Acad Sci U S A*. 2003;100:928–933.
8. Seidah NG, Mayer G, Zaid A, Rousselet E, Nassoury N, Poirier S, Essalmani R, Prat A. The activation and physiological functions of the proprotein convertases. *Int J Biochem Cell Biol*. 2008;40:1111–1125.
9. Benjannet S, Rhainds D, Essalmani R, Mayne J, Wickham L, Jin W, Asselin MC, Hamelin J, Varret M, Allard D, Trillard M, Abifadel M, Tebon A, Attie AD, Rader DJ, Boileau C, Brissette L, Chretien M, Prat A, Seidah NG. NARC-1/PCSK9 and its natural mutants: zymogen cleavage and effects on the low density lipoprotein (LDL) receptor and LDL cholesterol. *J Biol Chem*. 2004;279:48865–48875.
10. Maxwell KN, Fisher EA, Breslow JL. Overexpression of PCSK9 accelerates the degradation of the LDLR in a post-endoplasmic reticulum compartment. *Proc Natl Acad Sci U S A*. 2005;102:2069–2074.
11. Park SW, Moon YA, Horton JD. Post-transcriptional regulation of low density lipoprotein receptor protein by proprotein convertase subtilisin/kexin type 9a in mouse liver. *J Biol Chem*. 2004;279:50630–50638.
12. Surdo PL, Bottomley MJ, Calzetta A, Settembre EC, Cirillo A, Pandit S, Ni YG, Hubbard B, Sitlani A, Carfi A. Mechanistic implications for LDL receptor degradation from the PCSK9/LDLR structure at neutral pH. *EMBO Rep*. 2011;12:1300–1305.
13. Nassoury N, Blasiole DA, Tebon OA, Benjannet S, Hamelin J, Poupon V, McPherson PS, Attie AD, Prat A, Seidah NG. The cellular trafficking of the secretory proprotein convertase PCSK9 and its dependence on the LDLR. *Traffic*. 2007;8:718–732.
14. Lakoski SG, Lagace TA, Cohen JC, Horton JD, Hobbs HH. Genetic and metabolic determinants of plasma PCSK9 levels. *J Clin Endocrinol Metab*. 2009;94:2537–2543.
15. Dubuc G, Tremblay M, Pare G, Jacques H, Hamelin J, Benjannet S, Boulet L, Genest J, Bernier L, Seidah NG, Davignon J. A new method for measurement of total plasma PCSK9: clinical applications. *J Lipid Res*. 2010;51:140–149.
16. Poirier S, Mayer G, Benjannet S, Bergeron E, Marcinkiewicz J, Nassoury N, Mayer H, Nimpf J, Prat A, Seidah NG. The proprotein convertase PCSK9 induces the degradation of low density lipoprotein receptor (LDLR) and its closest family members VLDLR and ApoER2. *J Biol Chem*. 2008;283:2363–2372.
17. Shan L, Pang L, Zhang R, Murgolo NJ, Lan H, Hedrick JA. PCSK9 binds to multiple receptors and can be functionally inhibited by an EGF-A peptide. *Biochem Biophys Res Commun*. 2008;375:69–73.
18. Roubtsova A, Munkonda MN, Awan Z, Marcinkiewicz J, Chamberland A, Lazure C, Cianflone K, Seidah NG, Prat A. Circulating proprotein convertase subtilisin/kexin 9 (PCSK9) regulates VLDLR protein and triglyceride accumulation in visceral adipose tissue. *Arterioscler Thromb Vasc Biol*. 2011;31:785–791.
19. Abifadel M, Rabes JP, Devillers M, Munnich A, Erlich D, Junien C, Varret M, Boileau C. Mutations and polymorphisms in the proprotein convertase subtilisin kexin 9 (PCSK9) gene in cholesterol metabolism and disease. *Hum Mutat*. 2009;30:520–529.
20. Leren TP. Mutations in the PCSK9 gene in Norwegian subjects with autosomal dominant hypercholesterolemia. *Clin Genet*. 2004;65:419–422.
21. Timms KM, Wagner S, Samuels ME, Forbey K, Goldfine H, Jammulapati S, Skolnick MH, Hopkins PN, Hunt SC, Shattuck DM. A mutation in PCSK9 causing autosomal-dominant hypercholesterolemia in a Utah pedigree. *Hum Genet*. 2004;114:349–353.
22. Cunningham D, Danley DE, Geoghegan KF, Griffor MC, Hawkins JL, Subashi TA, Varghese AH, Ammirati MJ, Culp JS, Hoth LR, Mansour MN, McGrath KM, Seddon AP, Shenolikar S, Stutzman-Engwall KJ, Warren LC, Xia D, Qiu X. Structural and biophysical studies of PCSK9 and its mutants linked to familial hypercholesterolemia. *Nat Struct Mol Biol*. 2007;14:413–419.
23. Cohen J, Pertsemlidis A, Kotowski IK, Graham R, Garcia CK, Hobbs HH. Low LDL cholesterol in individuals of African descent resulting from frequent nonsense mutations in PCSK9. *Nat Genet*. 2005;37:161–165.
24. Zhao Z, Tuakli-Wosornu Y, Lagace TA, Kinch L, Grishin NV, Horton JD, Cohen JC, Hobbs HH. Molecular characterization of loss-of-function mutations in PCSK9 and identification of a compound heterozygote. *Am J Hum Genet*. 2006;79:514–523.

25. Hooper AJ, Marais AD, Tanyanyiwa DM, Burnett JR. The C679X mutation in PCSK9 is present and lowers blood cholesterol in a Southern African population. *Atherosclerosis*. 2007;193:445–448.
26. Dubuc G, Chamberland A, Wassef H, Davignon J, Seidah NG, Bernier L, Prat A. Statins upregulate PCSK9, the gene encoding the proprotein convertase neural apoptosis-regulated convertase-1 implicated in familial hypercholesterolemia. *Arterioscler Thromb Vasc Biol*. 2004;24:1454–1459.
27. Zaid A, Roubtsova A, Essalmani R, Marcinkiewicz J, Chamberland A, Hamelin J, Tremblay M, Jacques H, Jin W, Davignon J, Seidah NG, Prat A. Proprotein convertase subtilisin/kexin type 9 (PCSK9): Hepatocyte-specific low-density lipoprotein receptor degradation and critical role in mouse liver regeneration. *Hepatology*. 2008;48:646–654.
28. Piedrahita JA, Zhang SH, Hagaman JR, Oliver PM, Maeda N. Generation of mice carrying a mutant apolipoprotein E gene inactivated by gene targeting in embryonic stem cells. *Proc Natl Acad Sci U S A*. 1992;89:4471–4475.
29. Ishibashi S, Brown MS, Goldstein JL, Gerard RD, Hammer RE, Herz J. Hypercholesterolemia in low density lipoprotein receptor knockout mice and its reversal by adenovirus-mediated gene delivery. *J Clin Invest*. 1993;92:883–893.
30. Zhou YQ, Foster FS, Nieman BJ, Davidson L, Chen XJ, Henkelman RM. Comprehensive transthoracic cardiac imaging in mice using ultrasound biomicroscopy with anatomical confirmation by magnetic resonance imaging. *Physiol Genomics*. 2004;18:232–244.
31. Daugherty A, Whitman SC. Quantification of atherosclerosis in mice. *Methods Mol Biol*. 2003;209:293–309.
32. Whitman SC. A practical approach to using mice in atherosclerosis research. *Clin Biochem Rev*. 2004;25:81–93.
33. Plump AS, Smith JD, Hayek T, Aalto-Setala K, Walsh A, Verstuyft JG, Rubin EM, Breslow JL. Severe hypercholesterolemia and atherosclerosis in apolipoprotein E-deficient mice created by homologous recombination in ES cells. *Cell*. 1992;71:343–353.
34. Cohen JC, Boerwinkle E, Mosley TH Jr, Hobbs HH. Sequence variations in PCSK9, low LDL, and protection against coronary heart disease. *N Engl J Med*. 2006;354:1264–1272.
35. Herbert B, Patel D, Waddington SN, Eden ER, McAleenan A, Sun XM, Soutar AK. Increased secretion of lipoproteins in transgenic mice expressing human D374Y PCSK9 under physiological genetic control. *Arterioscler Thromb Vasc Biol*. 2010;30:1333–1339.
36. Véniant MM, Sullivan MA, Kim SK, Ambroziak P, Chu A, Wilson MD, Hellerstein MK, Rudel LL, Walzem RL, Young SG. Defining the atherogenicity of large and small lipoproteins containing apolipoprotein B100. *J Clin Invest*. 2000;106:1501–1510.
37. Seidah NG. PCSK9 as a therapeutic target of dyslipidemia. *Expert Opin Ther Targets*. 2009;13:19–28.
38. Poirier S, Mayer G, Poupon V, McPherson PS, Desjardins R, Ly K, Asselin MC, Day R, Duclos FJ, Witmer M, Parker R, Prat A, Seidah NG. Dissection of the endogenous cellular pathways of PCSK9-induced LDLR degradation: evidence for an intracellular route. *J Biol Chem*. 2009;284:28856–28864.
39. Twisk J, Gillian-Daniel DL, Tebon A, Wang L, Barrett PH, Attie AD. The role of the LDL receptor in apolipoprotein B secretion. *J Clin Invest*. 2000;105:521–532.
40. Blasiole DA, Oler AT, Attie AD. Regulation of ApoB secretion by the low density lipoprotein receptor requires exit from the endoplasmic reticulum and interaction with ApoE or ApoB. *J Biol Chem*. 2008;283:11374–11381.
41. Dietschy JM, Turley SD, Spady DK. Role of liver in the maintenance of cholesterol and low density lipoprotein homeostasis in different animal species, including humans. *J Lipid Res*. 1993;34:1637–1659.
42. Schmidt RJ, Beyer TP, Bensch WR, Qian YW, Lin A, Kowala M, Alborn WE, Konrad RJ, Cao G. Secreted proprotein convertase subtilisin/kexin type 9 reduces both hepatic and extrahepatic low-density lipoprotein receptors in vivo. *Biochem Biophys Res Commun*. 2008;370:634–640.
43. Luo Y, Warren L, Xia D, Jensen H, Sand T, Petras S, Qin W, Miller KS, Hawkins J. Function and distribution of circulating human PCSK9 expressed extrahepatically in transgenic mice. *J Lipid Res*. 2009;50:1581–1588.
44. Frank-Kamenetsky M, Grefhorst A, Anderson NN, Racie TS, Bramlage B, Akinc A, Butler D, Charisse K, Dorkin R, Fan Y, Gamba-Vitalo C, Hadwiger P, Jayaraman M, John M, Jayaprakash KN, Maier M, Nechev L, Rajeev KG, Read T, Rohl I, Soutschek J, Tan P, Wong J, Wang G, Zimmermann T, de Fougerolles A, Vornlocher HP, Langer R, Anderson DG, Manoharan M, Koteliansky V, Horton JD, Fitzgerald K. Therapeutic RNAi targeting PCSK9 acutely lowers plasma cholesterol in rodents and LDL cholesterol in nonhuman primates. *Proc Natl Acad Sci U S A*. 2008;105:11915–11920.
45. Gupta N, Fisker N, Asselin MC, Lindholm M, Rosenbohm C, Orum H, Elmen J, Seidah NG, Straarup EM. A locked nucleic acid antisense oligonucleotide (LNA) silences PCSK9 and enhances LDLR expression in vitro and in vivo. *PLoS ONE*. 2010;5:e10682.
46. Chan JC, Piper DE, Cao Q, Liu D, King C, Wang W, Tang J, Liu Q, Higbee J, Xia Z, Di Y, Shetterly S, Arimura Z, Salomonis H, Romanow WG, Thibault ST, Zhang R, Cao P, Yang XP, Yu T, Lu M, Retter MW, Kwon G, Henne K, Pan O, Tsai MM, Fuchslocher B, Yang E, Zhou L, Lee KJ, Daris M, Sheng J, Wang Y, Shen WD, Yeh WC, Emery M, Walker NP, Shan B, Schwarz M, Jackson SM. A proprotein convertase subtilisin/kexin type 9 neutralizing antibody reduces serum cholesterol in mice and nonhuman primates. *Proc Natl Acad Sci U S A*. 2009;106:9820–9825.
47. Abifadel M, Pakradouni J, Collin M, Samson-Bouma ME, Varret M, Rabes JP, Boileau C. Strategies for proprotein convertase subtilisin kexin 9 modulation: a perspective on recent patents. *Expert Opin Ther Pat*. 2010;20:1547–1571.

CLINICAL PERSPECTIVE

The proprotein convertase subtilisin/kexin type 9 (PCSK9) promotes the degradation of the low-density lipoprotein receptor and hence is a promising target to treat hypercholesterolemia and to prevent cardiovascular diseases. Clinical trials are currently under way to determine whether inhibiting PCSK9 is a safe and efficient approach in humans. The present study demonstrates for the first time that the absence of PCSK9 protects both wild-type and apolipoprotein E–deficient mice from atherosclerosis. This protection is dependent on the low-density lipoprotein receptor because the correlation between PCSK9 and atherosclerosis was lost in low-density lipoprotein receptor–deficient mice. Our data thus suggest that PCSK9 inhibition will be beneficial in reducing the development of atherosclerosis. In view of the selectivity of action of PCSK9 on the low-density lipoprotein receptor in the liver and possibly in the small intestine, it is expected that drugs that would target PCSK9 will exhibit fewer side effects than those related to statins.

Gene Inactivation of Proprotein Convertase Subtilisin/Kexin Type 9 Reduces Atherosclerosis in Mice

Maxime Denis, Jadwiga Marcinkiewicz, Ahmed Zaid, Dany Gauthier, Steve Poirier, Claude Lazure, Nabil G. Seidah and Annik Prat

Circulation. 2012;125:894-901; originally published online January 18, 2012;
doi: 10.1161/CIRCULATIONAHA.111.057406
Circulation is published by the American Heart Association, 7272 Greenville Avenue, Dallas, TX 75231

Print ISSN: 0009-7322. Online ISSN: 1524-4539

SUPPLEMENTAL MATERIAL

Supplemental Methods

Immunoprecipitation of plasma PCSK9. Circulating mouse PCSK9 levels were analyzed by immunoprecipitation (IP) using the TrueBlot system (eBioscience). Briefly, 60 µL of pooled plasma (3 x 20 µL) were incubated as previously described[1] with 3µL of a mouse PCSK9 antibody[2] and 50µl of TrueBlot anti-rabbit Ig IP beads. Samples were then centrifuged at 7000 rpm for 1 min and washed with 0.5 x RIPA (100 mM Tris-HCl pH 8, 300 mM NaCl, 0.2% SDS, 2% NP-40, 0.5% Na-deoxycholate) buffer for six times. Immunoprecipitated PCSK9 (30 µL) was resolved by 10% SDS-PAGE and blotted on a HyBond nitrocellulose membrane (GE Healthcare), which was blocked for 1 h in TBS-T (50mM Tris-HCl, pH 7.5, 150 mM NaCl, 0.1% Tween-20) containing 5% nonfat dry milk. Membranes were incubated with mouse PCSK9 antibody[2] (1:2500) for 3 h at room temperature (RT), and then with TrueBlot anti-rabbit horseradish peroxidase-conjugated secondary antibody (1:2500) for 1 h at RT. Detection was performed using an ECL plus kit (GE Healthcare).

Immunoblots from liver tissue. About 10 mg of liver tissue were homogenized using polytron in 2 mL of 1 x RIPA buffer supplemented with 1 x Complete Protease Inhibitor Mixture. Proteins (75 µg) were separated by 10% SDS-PAGE and blotted on a HyBond nitrocellulose membrane (GE Healthcare), which was blocked for 1 h in TBS-T containing 5% nonfat dry milk. Membranes were then incubated with mouse LDLR (1:1000; R&D Systems), SR-BI (1:1500; Novus Biologicals) or β-actin (1:4000; Sigma-Aldrich) antibodies for 3 h at RT followed by incubation with corresponding horseradish peroxidase-conjugated secondary antibodies (1:10000) at RT for 1 h. Specific bands were detected with enhanced an ECL plus kit (GE Healthcare).

ELISA for quantification of PCSK9 from plasma. Murine PCSK9 was measured using the kit from Circulex (cat no CY-8078) according to the manufacturer's instructions. Briefly, plasma was diluted 1:100 with the provided buffer and 100 µL of diluted plasma were loaded/well. In order to fit in the linear range of the standard curve, plasma from mice that exhibit high circulating PCSK9 levels (Tg and LDLR-deficient) were further diluted 60 x prior to loading on the 96-well plate.

Supplemental Table: Primers used for the genotyping of mice

Technique	Gene	Sense	Primer sequence	Allele	Fragment size
PCR	*Apoe*	Forward	FAM – GCCTAGCCGAGGGAGAGCCG		
		Reverse	TGTGACTTGGGAGCTCTGCAGC	WT	155 bp
		Reverse	GCCGCCCCGACTGCATCT	KO	250 bp
	Ldlr	Forward	VIC – CCATATGCATCCCCAGTCTT		
		Reverse	AATCCATCTTGTTCAATGGCCGATC	WT	167 bp
		Reverse	GCGATGGATACACTCACTGC	KO	350 bp
	Pcsk9	Forward	FAM – ACTCCCCACAACTACGGACTGT		
		Reverse	ATCTTTCAGGATGCTGCATTT	WT	213 bp
		Reverse	CATCCCTTTAGGCACAGAGCTT	KO	338 bp
qPCR	*Tg(PCSK9-V5)*	Forward	TGT GTG TGG CAA GAG TCC ATG ACA		
		Reverse	AGG AGA GGG TTA GGG ATA GGC TTA		142 bp
		Probe	FAM - CTC CTG GGT TCA GAC CG		

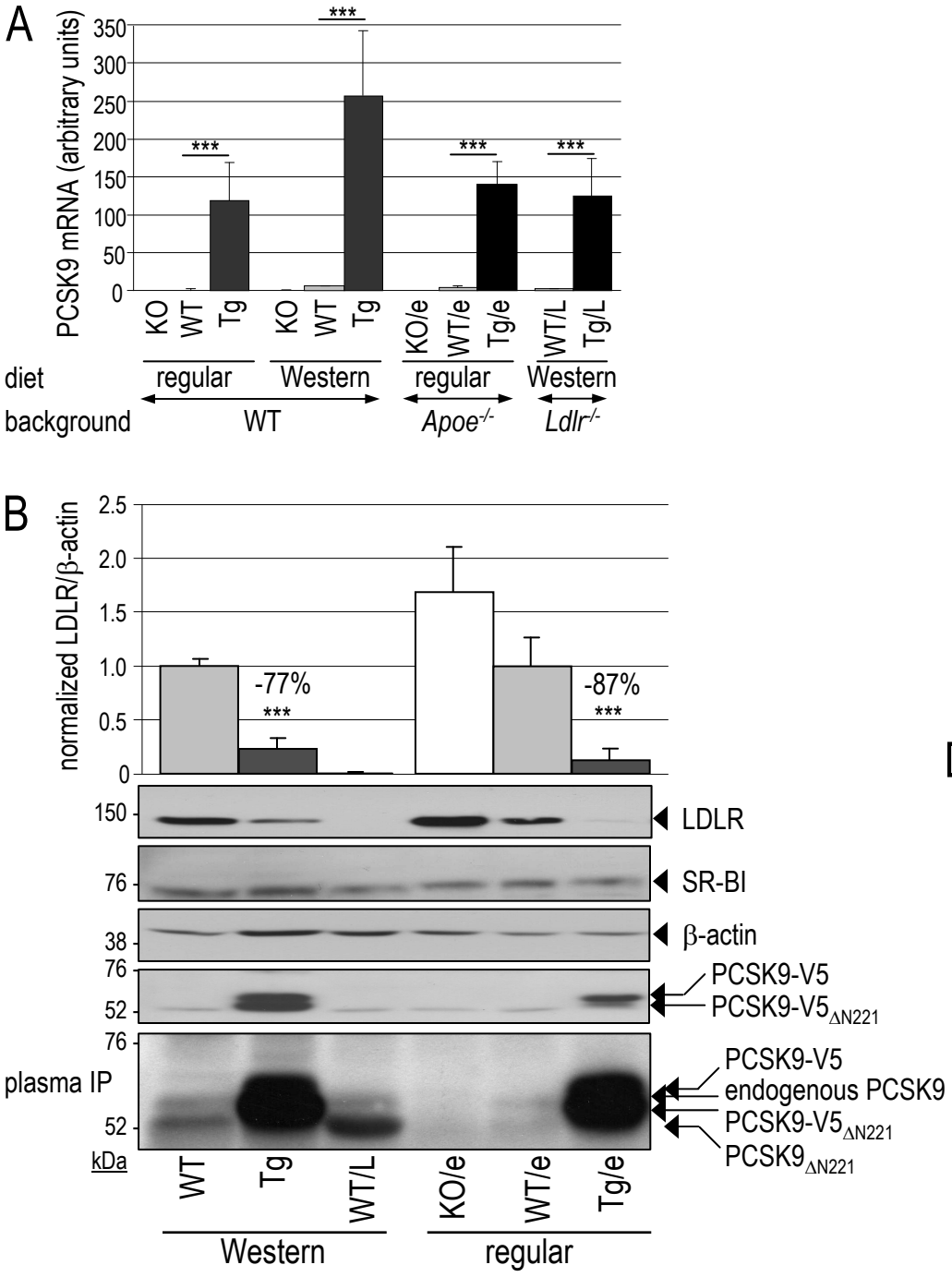

Supplemental Figure 1

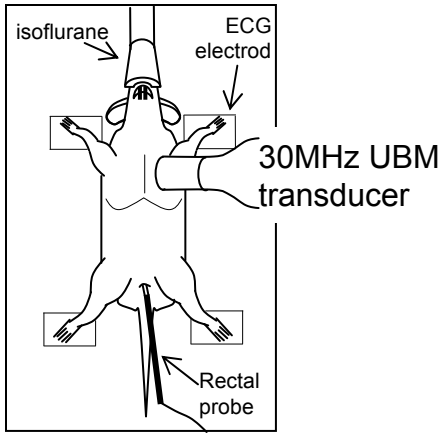

left parasternal long-axis

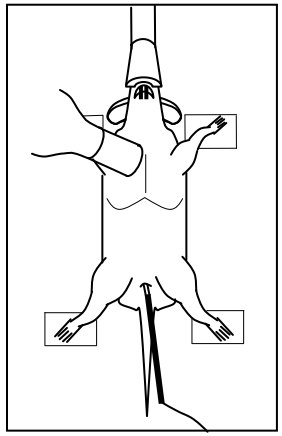

right parasternal short-axis

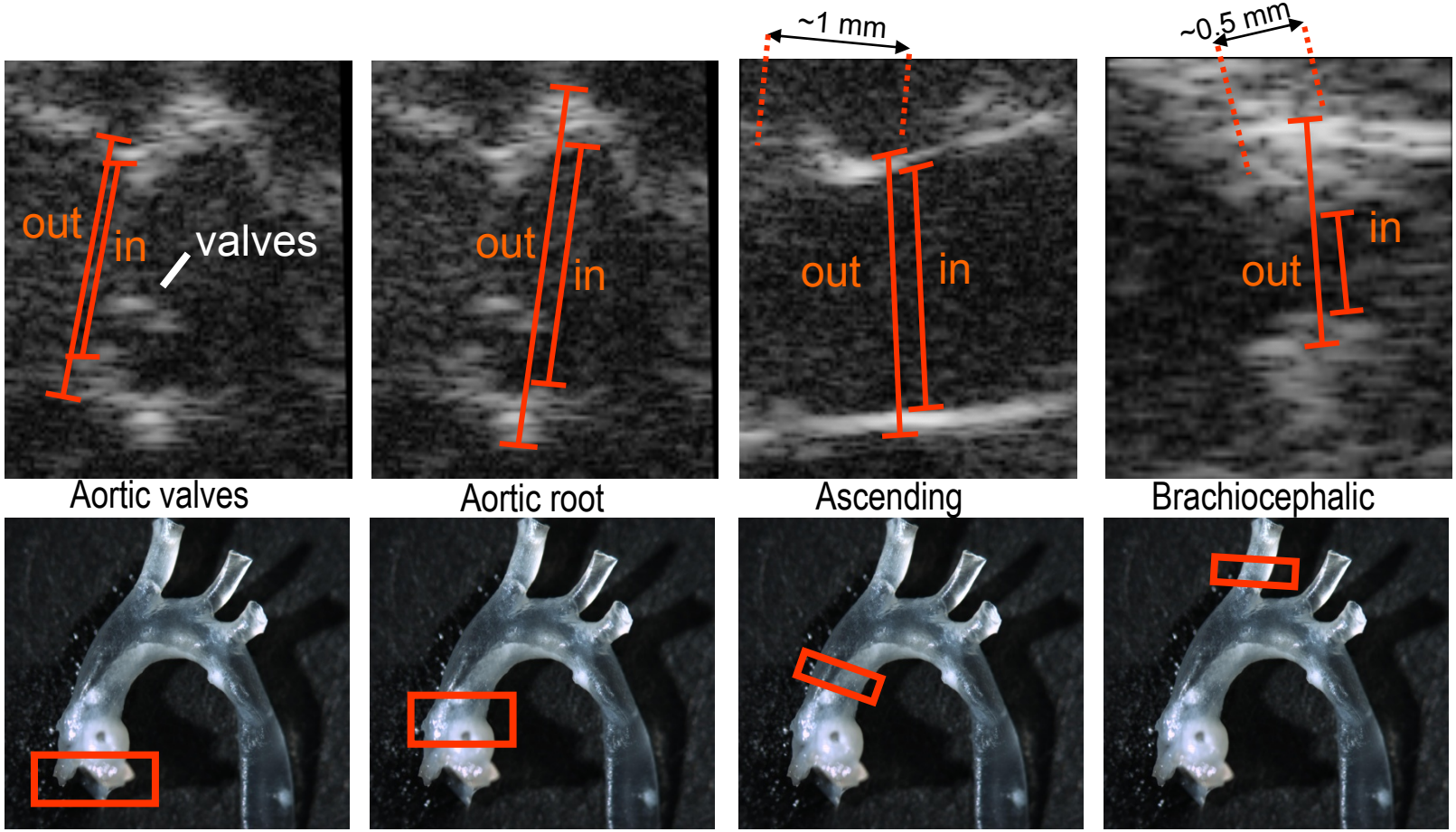

Supplemental Figure 2

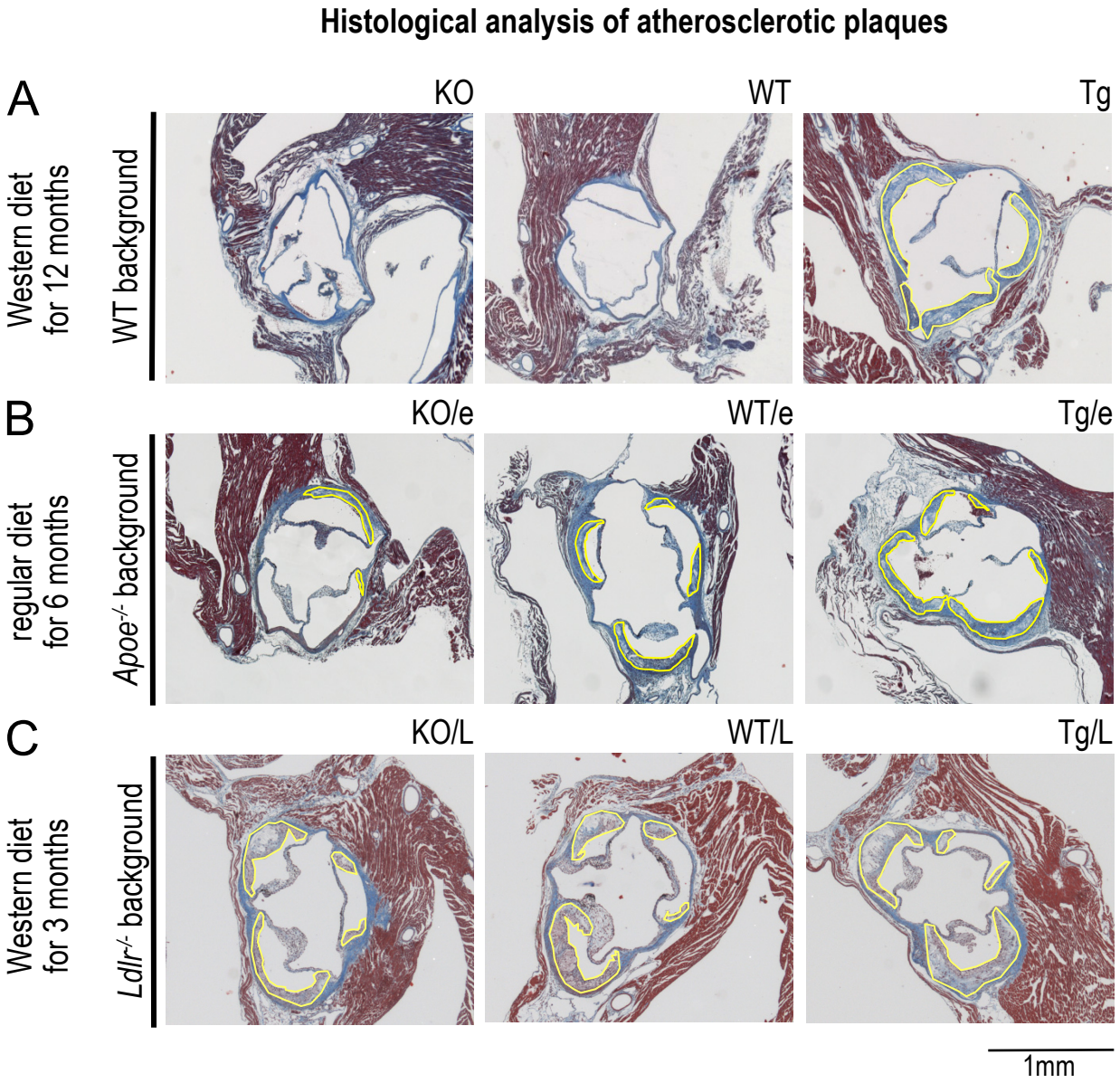

Supplemental Figure 3

Effect of gender in apoE-deficient mice fed a regular diet for 6 months

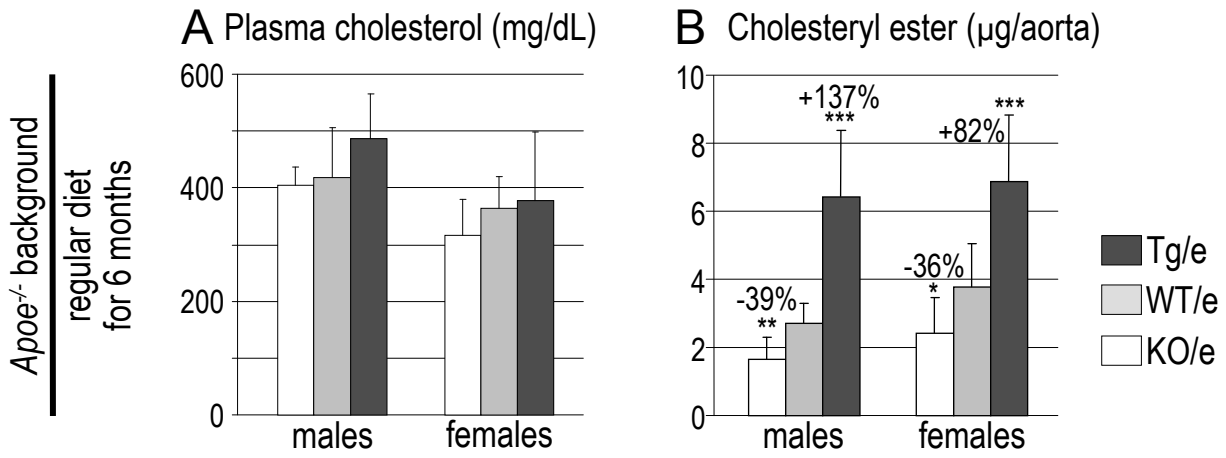

Supplemental Figure 4

ApoE-deficient mice fed a Western diet for 6 months

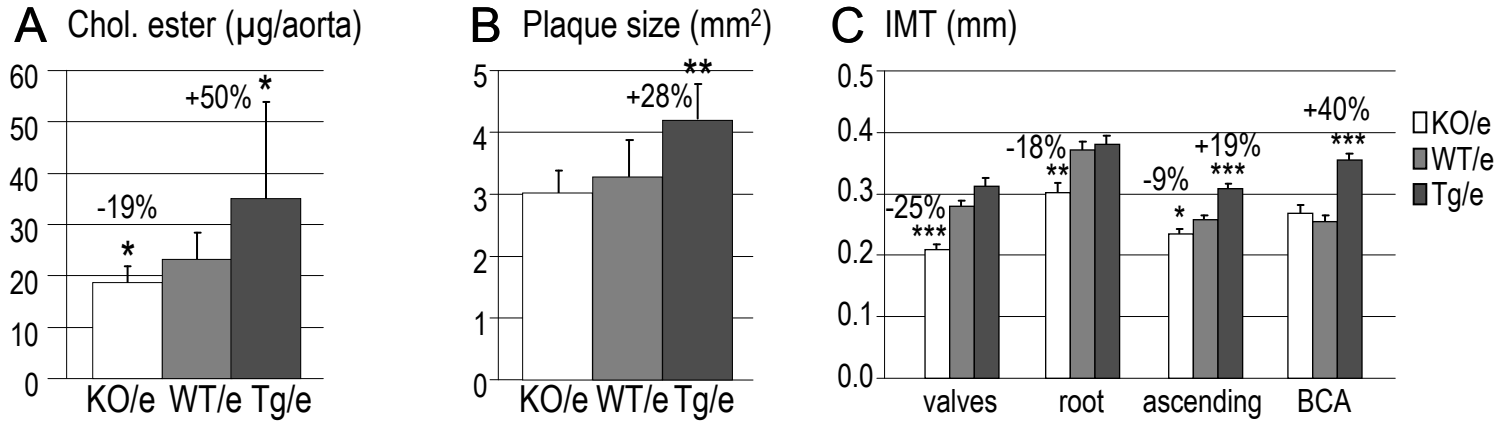

Supplemental Figure 5

Tg versus *Ldlr*$^{-/-}$ mice on Western diet for 6 months

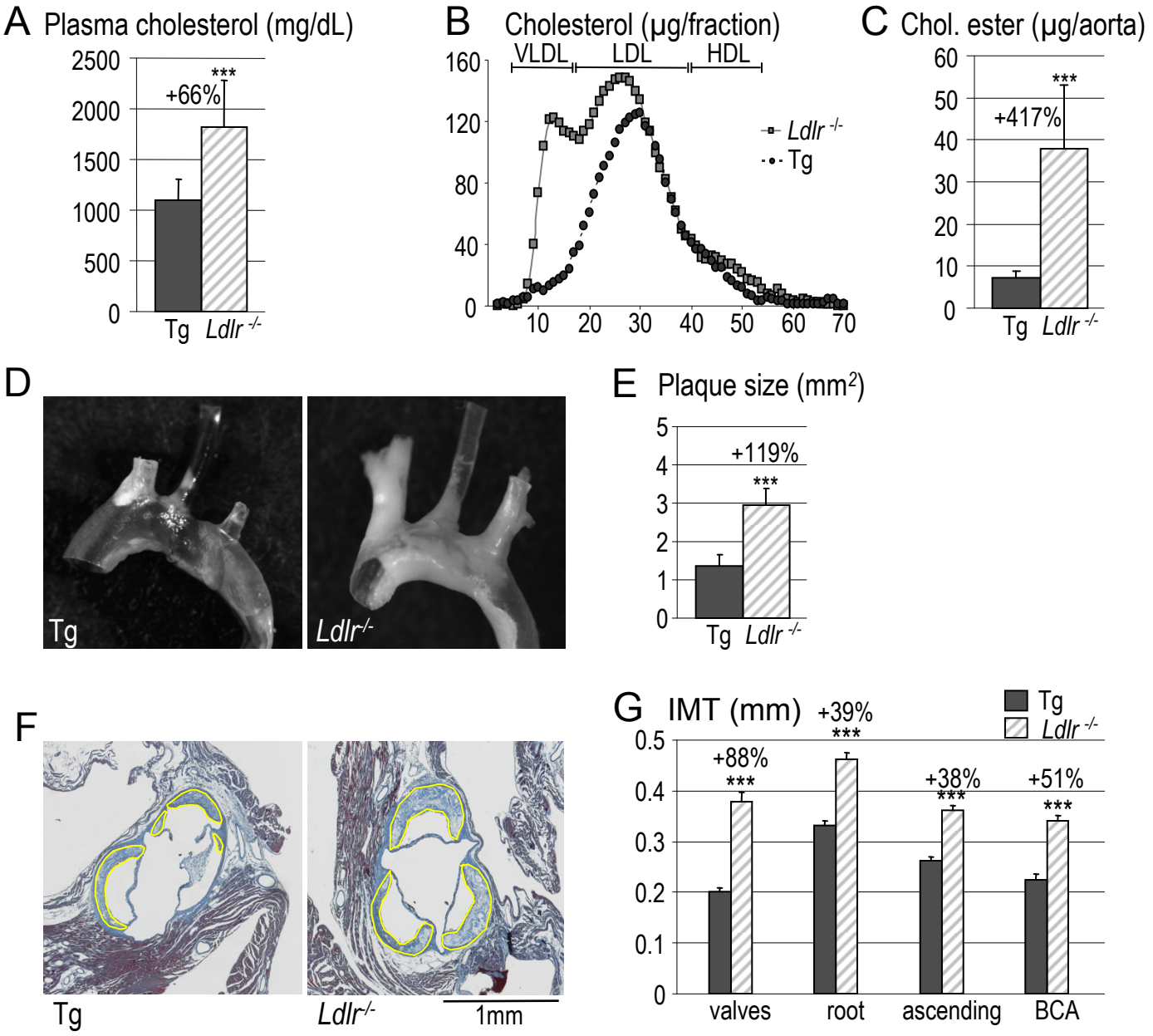

Supplemental Figure 6

Supplemental Figure legends

Supplemental Figure 1: Characterization of mice used in this work. A, QPCR quantification of PCSK9 mRNA in liver tissue from different mouse lines (5 mice/group). B, SDS-PAGE of pools of 3 liver extracts from WT, Tg or LDLR-deficient mice (WT/L) that were fed a Western diet for 6 months (left wells) or apoE-deficient mice expressing no (KO/e), normal (WT/e), or high (Tg/e) levels of PCSK9 that were fed a regular diet for 6 months (right wells). Immunoblotting with LDLR, SR-BI, β-actin, V5 or murine PCSK9 (plasma immunoprecipitation) primary antibodies. *Top graph*: Quantification of the LDLR signal normalizes to β-actin (n = 3). C, PCSK9 ELISA performed on diluted plasma samples (n = 4 to 6). D, LDLR immunohistochemistry performed as previously described[3] on liver cryosections. LDLR is visualized in green and nuclei in blue (Hoechst's staining). Bars and error bars represent mean + SD. By comparison with corresponding WT values (grey bars), *P* (***, ≤ 0.001) was obtained by a two-tailed Student's *t*-test.

Supplemental Figure 2: Graphical representation of the ultrasound biomicroscopy technique used for the determination of intima-media thickness. A Vevo 770 apparatus (Visual Sonics, Toronto, Canada) equipped with a 30 MHz probe was utilized to determine IMTs. A left parasternal long-axis view was used to visualize aortic valves, aortic root and ascending aorta, whereas a right parasternal short-axis view allowed visualization of the brachiocephalic artery. "In" and "out" measurements served to determine IMT as described in the Method section.

Supplemental Figure 3. Histological analysis of atherosclerotic plaques. Atherosclerotic plaques were outlined in sections at the level of valves that were stained with Masson's trichrome. A, KO, WT and Tg mice fed a Western diet for 12 months; B, apoE-deficient mice expressing either no PCSK9 (KO/e), normal (WT/e), or high (Tg/e) levels of PCSK9 and fed a regular diet for 6 months; C, LDLR-deficient mice expressing either no PCSK9 (KO/L), normal (WT/L), or high (Tg/L) levels of PCSK9 and fed a Western diet for 3 months.

Supplemental Figure 4: The modulation of aortic cholesteryl ester accumulation by PCSK9 is not gender-dependent. Male and female apoE-deficient mice that express either no PCSK9 (KO/e), normal (WT/e) or high (Tg/e) levels of PCSK9 were fed a regular diet for 6 months. At sacrifice, total plasma cholesterol (A) (n = 8 to 18) and CE content of the aorta (B) (n = 8 to 15) were determined. Bars and error bars represent average + SD. By comparison with WT/e values, *P* (*, ≤ 0.05; **, ≤ 0.01; ***, ≤ 0.001) was obtained by a two-tailed Student's *t*-test.

Supplemental Figure 5: PCSK9-deficiency prevents atherosclerosis in apoE-deficient mice fed a Western diet. ApoE-deficient mice in which PCSK9 was either knocked out (KO/e), wild-type (WT/e) or overexpressed (Tg/e) were fed a Western diet for 6 months. A, CE accumulation in the whole aorta (n = 5 to 12); B, surface occupied by plaques at the level of aortic valves and root (n = 10 to 12); C, intima/media thickness (IMT) determined by ultrasound biomicroscopy at the level of valves, root, ascending aorta and brachiocephalic artery (BCA) (n = 13 to 16). Bars and error bars represent average + SD. By comparison with WT/e values, *P* (*, ≤ 0.05; **, ≤ 0.01; ***, ≤ 0.001) was obtained by a two-tailed Student's *t*-test.

Supplemental Figure 6: High expression of PCSK9 only partially mimics the LDLR-deficient phenotype. Tg and LDLR-deficient mice (*Ldlr*$^{-/-}$) were fed a Western diet for 6 months. A, plasma cholesterol (n = 6 to 12); B, FPLC cholesterol profiles (pooled plasma from 6 to 10 mice/genotype); C, CE accumulation in the whole aorta (n = 6 to 12); D, representative en face preparations of aortic arches; E, cumulative plaque surface at the level of aortic valves and root (n = 9 to 11); F, atherosclerotic plaques outlined in sections at the level of valves stained with

Masson's trichrome; G, IMT at the level of aortic valves and root, ascending aorta and brachiocephalic artery (BCA) by ultrasound biomicroscopy (n = 10 to 12). Average + SD, except in F, where average + SEM. ***, $P \leq 0.001$.

Supplemental References

(1) Essalmani R, Susan-Resiga D, Chamberland A, Abifadel M, Creemers JW, Boileau C, Seidah NG, Prat A. In vivo evidence that furin from hepatocytes inactivates PCSK9. *J Biol Chem.* 2011;286:4257-4263.

(2) Nassoury N, Blasiole DA, Tebon OA, Benjannet S, Hamelin J, Poupon V, McPherson PS, Attie AD, Prat A, Seidah NG. The Cellular Trafficking of the Secretory Proprotein Convertase PCSK9 and Its Dependence on the LDLR. *Traffic.* 2007;8:718-732.

(3) Zaid A, Roubtsova A, Essalmani R, Marcinkiewicz J, Chamberland A, Hamelin J, Tremblay M, Jacques H, Jin W, Davignon J, Seidah NG, Prat A. Proprotein convertase subtilisin/kexin type 9 (PCSK9): Hepatocyte-specific low-density lipoprotein receptor degradation and critical role in mouse liver regeneration. *Hepatology.* 2008;48:646-654.